EARTH SCIENCES
RESEARCH JOURNAL

Earth Sci. Res. J. Vol. 9, No. 2 (Dec. 2005): 148-164

THE PAIPA VOLCANO, EASTERN CORDILLERA OF COLOMBIA, SOUTH AMERICA (PART II): PETROGRAPHY AND MAJOR ELEMENTS PETROLOGY

Natalia Pardo Villaveces[1], José María Jaramillo[2], Héctor Cepeda[3]

[1] Universidad Nacional de Colombia. POBox 101130 Bogotá, Colombia. E-mail:azufralrouge@yahoo.es
[2] Latin America Enterprise Fund Managers L.L.C E-mail: jjaramillo@laef.co
[3] Geological Survey of Colombia (INGEOMINAS- Bogota). E-mail: hcepeda@ingeomin.gov.co

RESUMEN

Los productos del volcán de Paipa (Pardo et al., 2005) son principalmente depósitos de flujos piroclásticos de pómez y ceniza, domos y flujos pirolásticos de bloques y ceniza. Se trata de riolitas alcalinas, traquitas alcalinas y riolitas calcoalcalinas altas en Potasio. Los datos químicos evidencian contenidos de SiO2 entre 68 y 72%, y de álcalis (Na2O+K2O) entre 7%-10%. Los minerales esenciales son fenocristales y glomerocristales de anortoclasa, sanidina hasta de 1,5 cm y anortoclasas con núcleos de plagiocalasa; los minerales accesorios son biotita roja y hastingsita, mientras que los traza son augita, circón, esfena y magnetita. Los cristales presentan texturas de desequilibrio, tal como bahías de disolución, bordes de corrosión y reabsorción, zonación normal, inversa, oscilatoria y en parches, así como bordes euhedrales intercalados con bordes fibrosos. En correlación con datos publicados sobre las rocas volcánicas de Iza, la geoquímica de elementos mayors de las rocas volcánicas de Paipa indican que los magmas alcalinos y ácidos que hicieron erupción en la Cordillera Oriental de Colombia durante el Neógeno son distintos a los magmas calcoalcalinos que hacen actualmente erupción en el arco activo de la Cordillera Central de Colombia. Aún hacen falta estudios detallados de la geología structural, geoquímica y geofísica para establecer el ambiente geodinámico que gobierna el vulcanismo Plio-Pleistoceno en la Cordillera Oriental.

Palabras clave: Composición modal, composición normal, domos, erupción freatomagmática, flujos piroclásticos, ignimbritas, norma CIPW, textura de pared de burbuja, pyroclastic flows, shards.

ABSTRACT

Paipa volcano products are mainly pyroclastic pumice and ash flow tuffs, lava domes and pyroclastic block and ash flow tuffs. They are classified as alkaline rhyolites and trachytes and high-K calcalkaline rhyolites. Chemical data show SiO_2 values between 68 and 72%, and alkalis (Na_2O+K_2O) content of 7%-10%. Essential minerals are phenocrysts and glomerocrysts of anorthoclase, sanidine up to 1,5 cm and anorthoclase-mantled

(Manuscript received march 2005
Paper accepted October 2005)

plagioclase; accessory minerals are red biotite, and hastingsite while trace minerals are augite, zircon, sphene and magnetite. Crystals have disequilibrium textures, such as dissolution embayments, corrosion and reabsortion borders, normal, inverse, oscillating and patchy zonation, together with fibrous borders intercalated with euhedral borders. In correlation with published data of Iza volcanic rocks, Paipa rocks chemical composition confirms that acid and alkaline magmas that have erupted in the Eastern Cordillera of Colombia during the Neogene are strongly different from the calc-alkaline magmas that erupt in the westward active arc (Central Cordillera). Detailed structural, geochemical and geophysical research has to be done in future research to establish the geodynamic framework that governs the volcanism of the Eastern Cordillera.

Key words: Bubble-wall texture, CIPW norm, ignimbrites, lava-domes, phreatomagmatic eruptions, pyroclastic flows, modal compositions, normal composition, shards

INTRODUCTION

The Paipa volcano is located at the central part of the Eastern Cordillera of Colombia (EC), in the Department of Boyaca (Figure 1). It has a 3 km diameter caldera possibly related to the interaction of NE high angle faults parallel to the principal structures of the EC, which are mainly inverse with left-lateral component, and NW normal faults that cut the regional structures (Pardo-Villaveces et al., 2005).

Pardo-Villaveces (2004) defined 14 eruptive units within two eruptive epochs: during the First Eruptive Epoch (FEE) a volcanic caldera was formed and its final collapse occurred at the end. After a quiescence period, caldera resurgence occurred during the Second Eruptive Epoch (SEE) with the formation of several vents inside it, most of them located at Olitas headstream; lava domes, block and ash flow deposits, pyroclastic surges and ignimbrites interbedded with lacustrine siltstones and torrential oligomictic conglomerates remained restricted to the caldera depression, while ash fall tuffs mantled inflow and outflow zones (Figure 2)(Cepeda & Pardo-Villaveces 2004; Pardo-Villaveces et al., 2005). A Pliocene and possibly Pleistocene age was determined by Ar/Ar and K/Ar radiometric methods: Ar/Ar analysis gave ages between 2,1 and 2,4 Ma for the lava domes that were formed at the beginning of the SEE, while K/Ar methods gave a 1,8 Ma date for crystalline flow tuffs accumulated westward from the domes during the SEE also (Cepeda et al., 2004; Pardo-Villaveces 2004; Cepeda & Pardo-Villaveces 2004; Pardo-Villaveces et al., 2005).

Optical petrography and major elements geochemical data are here presented to illustrate the composition of Paipa volcano products and to give an initial approach to some of the processes that possibly occurred during magma ascent and eruption.

METHODOLOGY

During the field work (Pardo-Villaveces et al., 2005), we selected 19 samples for petrographic analysis, based on the minimal grade of meteorization and hydrothermal alteration; sites of sample selection are localized on the geologic map shown in Figure 2. Pyroclastic rocks were classified according to Wohletz & Heiken (1992) diagram. Modal composition was given based on the phenocrist assemblage of each rock, together with their detailed description based on hand samples and thin sections. Amphibole, biotites and feldspar compositions were determined by optical properties, such as relief, pleochroic colors, 2v angle amplitude, birefringence, extinction angles, optic figure and sign; for twinned plagioclase Michel-Levy plagioclase-determination method was used.

Based on petrography observations we selected five samples for total rock major elements chemical analysis that was done in INGEOMINAS-Bogotá laboratory. Chemical classification was given by TAS diagram (Le Maitre, 1989) and CIPW norm was calculated using Norma.xsl. These data were correlated with other 10 data obtained by INGEOMINAS Colombia geochemical map project to support our observations (Cepeda & Pardo-

Villaveces, 2004). The petrologic interpretations and suggestions here presented are based on the 15 major oxides geochemical data and the following results are based on the volcanic stratigraphy determined and discussed in Pardo-Villaveces et al. (2005).

RESULTS

Unit I.1 samples: the oldest ash flow tuff deposit was sampled in PPG-057 and PPG059 stations (Figure 2). Hand samples are white to red dense and welded pyroclastic rocks, poorly sorted, with up to 40 % of anorthoclase (Kfs) and sanidine (Sa) phenocrystals in a vitric-clastic ash matrix. Feldspar crystals are oriented and aligned, giving a flow texture to the rocks, and are as large as 1,5 cm (Figure 3). Lithic fragments are accidental block-sized silicic and phosphoric siltstones, chert, green and gray phylites, rarely founded in finer sizes. In thin section (Figure 4) these rocks were classified as crystalline-vitric to crystalline pyroclastic flow tuffs (Table 1, Figure 5). Phenocrysts are aligned in a vitrophiric matrix with occasional blocky shards and pumice fragments with chipped edges. Essential minerals are anorthoclase and sanidine free crystals and glomerocrysts. Most of the anorthoclase is presented as poikilocryst with a plagioclase nucleus that presents reabsortion borders (Figure 4). Free plagioclase is oligoclase in composition and it is often zoned or twinned. Accessory and trace minerals are corroded and oxidized hastingsite (Figure 6), euhedral zircon and euhedral sphene. Rocks are K-feldspar trachytes determined by modal classification.

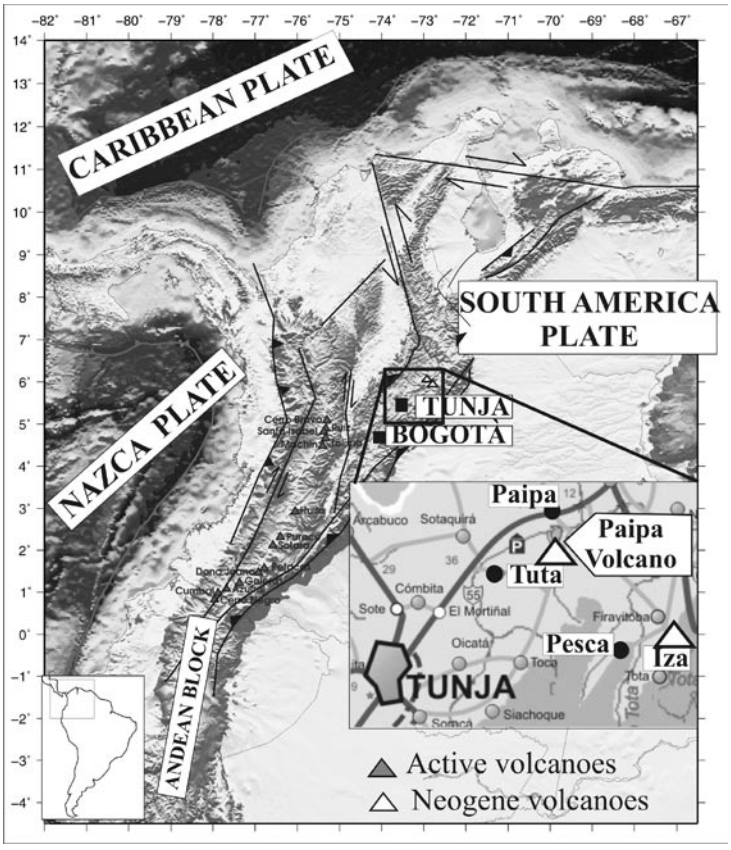

Figure 1. The Paipa volcano is located at the Eastern Cordillera of Colombia, eastward of the active arc (Pardo-Villaveces et al., 2005).

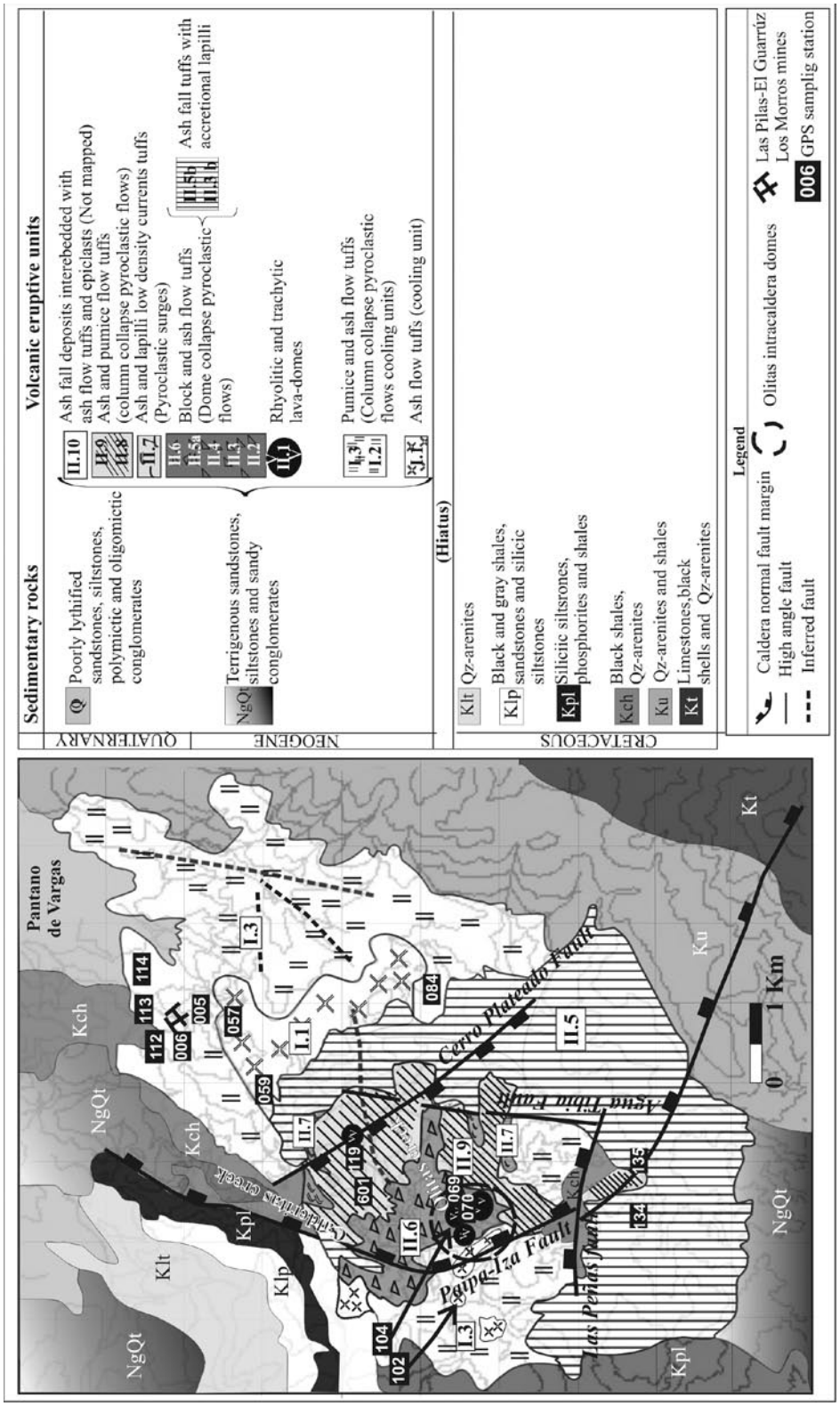

Figure 2. Geologic map of Paipa volcano products (Pardo-Villaveces et al., 2005).

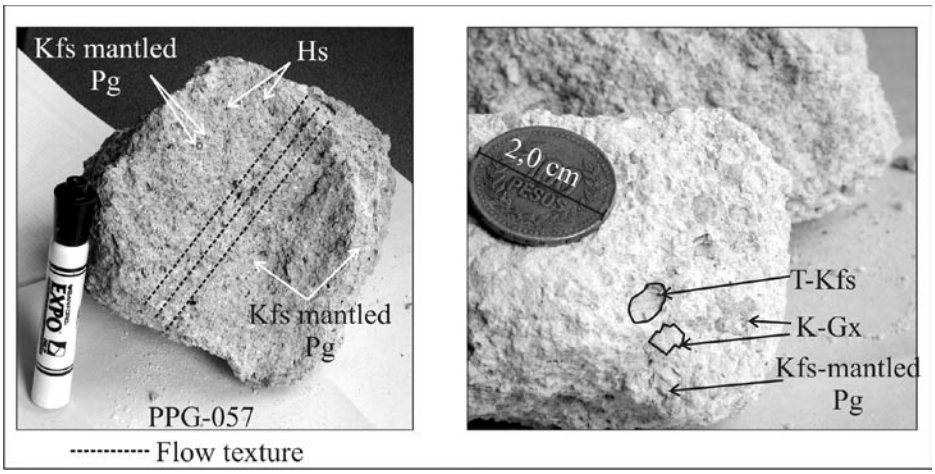

Figure 3. A. Hand sample of unit I.1 outcropping at GPS station PPG-057. Juvenile fragments are anorthoclase, plagioclase, sanidine and hastingsite fractured crystals. Rocks show a flow texture by crystals alignment. B. Plagioclase is often mantled by an anorthoclase rims while K-feldespars are clustered in glomeroporphyritic textures. Kfs-mantled Pg = anorthoclase-mantled plagioclase; K-Gx = K-feldespar glomerocrysts; Hs = hastingsite; T-Kfs = twinned anorthoclase.

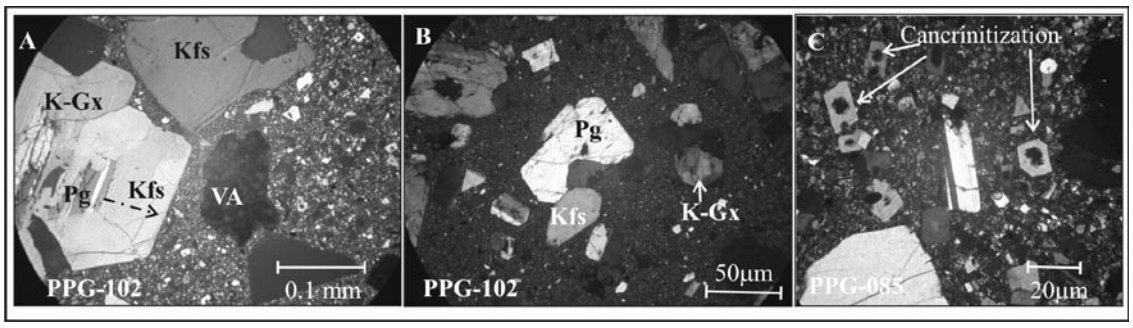

Figure 4. Pyroclastic vitric-crystalline texture of unit I.1 flow tuffs. A. Feldespar juvenile crystals, glomerocrystals and poikilocrystals together with subangular volcanic accessory lithics are embedded in a vitroclastic matrix with flow texture. B.
K-□
K-□
K-feldspar glomerocryst; Pg = plagioclase (oligoclase).

Unit I.2 samples: this pumice and ash flow cooling unit was sampled in PPG-006 and PPG-084 GPS stations (Figure 2). Hand samples are poorly sorted pyroclastic flow tuffs, moderately welded, with 30% of block and lapilli-sized juvenile pumice fragments; there are also accessory pumice fragments and accidental red, yellow and gray siltstones, cherts, red, yellow, white and green phylites, black schists and quartzites in a yellow to brown ash and pumice matrix (Figure 8). Micro-textures (Figure 9) are vitric-crystalline (Table 1, Figure 5), with pumice fragments of different cristallinity in a glassy matrix with abundant bubble-wall shards and pumice. Juvenile crystals are the same as in unit I.1 samples, with dominating sanidine crystals, anorthoclase glomerocrysts and poikilocrysts (Figure 10). Rocks were classified as K-feldspar trachytes on modal observations (Table 1), but sample PPG-084i chemical composition suggests high-K calc-alkaline rhyolites (Table 2, Figure 7).

TABLE 1. 100% NORMALIZED SOLIDS PERCENTAGE (I.E. WITHOUT GLASS), TEXTURAL AND MODAL CLASSIFICATIONS ARE SHOWN, BASED ON STRECKEISEN (1978) CLASSIFICATION. KFS= ANORTOCLASE; SA= SANIDINE; PL= PLAGIOCLASE (OLIGOCLASE-ANDESINE); HS=HASTINGSITE; OXHNB= OXIHORNBLENDE; BT= BIOTITE; TI-BT=TITANOBIOTITE; AUG= AUGITE-AEGIRINE; TTN= SPHENE; ZR= ZIRCON; OP= OPACH MINERALS. CI= CRYSTALLIZATION INDEX; J=JUVENILE FRAGMENTS; NJ= NOT-JUVENILE FRAGMENTS.

SAMPLE	057	057j	085	102	102j	006	PV3j	005E	005D	112	113	114	071	104	070	069	69j	119	119j
Kfs	47	38	38	45	46	53	14	58	41		40	83		70	60	31	62	72	64
Sa	19	38	42	39	25	32	68	12	44	88	27	7	81		8	29	8		14
Pl	4	13	4	13	9	5	5	4	3	13	13	3		5	4	6	8	10	4
Hs	20	16	6					8						3	4	7		7	7
Oxhorn														2					4
Bt	2		2		5	8		4	6					10	16	1	14	4	5
Ti-bt														6	1	20	1		
Aug																			2
Ttn				3	4						20	3			2	1	1	2	
Zr	4	7	4		4	3	9	15	6				6	1		2	1	3	
Op	7				7		5					3	13	4	4	4	3	1	
CI	44	53	57	38	48	24	17	20	23	2	7	17	18	92	69	58	53	48	44
J	99	99	99	97	99	92	98	88	97	88	93	98	90						
NJ	1	1	1	2	1	8	2	12	3	12	7	2	10						
Textural classification	Cyistal-vitric	Cyistal-vitric	Cyistal-vitric	Cyistal-vitric	Cyistal-vitric	Vitric-cystalline	Vitric-crystalline	Vitric-lithic	Vitric-crystalline	Vitric-lithic	Vitric	Vitric-crystalline	Vitric-crystalline	Hypocrystalline porphyritic, with 2 Kfs generations, glomerocrysts and Kfs poikylocrysts				Hypohialine Porphyritic	
Modal classification	K-feldspar trachyte	K-feldspar trachyte	K-feldspar trachyte	Trachyte	Trachyte	K-feldspar trachyte	K-feldspar trachyte	K-feldspar trachyte	K-feldspar trachyte	Trachyte	Trachyte	K-feldspar trachyte	K-feldspar trachyte	Red biotita bearing K-feldspar trachyte			Trachyte	K-feldspar trachyte	

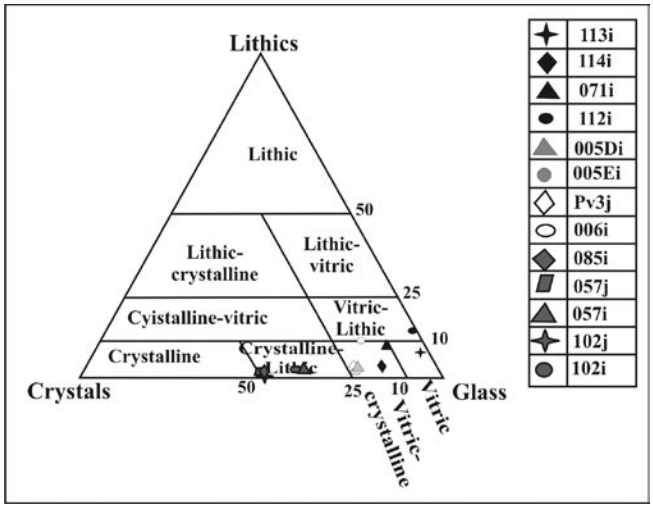

Figure 5. Textural classification of pyroclastic rocks.

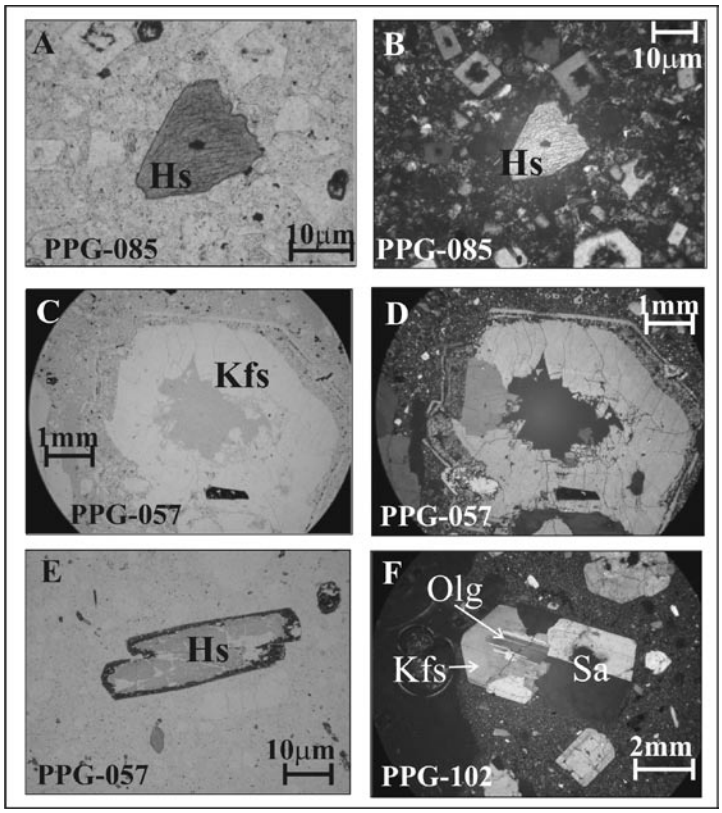

Figure 6. A-B. Hastingsite phenocrystal with dissolution embayments. C-D. Anorthoclase phenocrystal with hollow nucleus and disequilibrium rims. E. Hastingsite altered to chlorite and borders are often corroded and oxidized. F. Anorthoclase poikilocrysts wi□
Hs = hastingsite; Kfs = anorthoclase; Olg = oligoclase; Sa = sanidine.

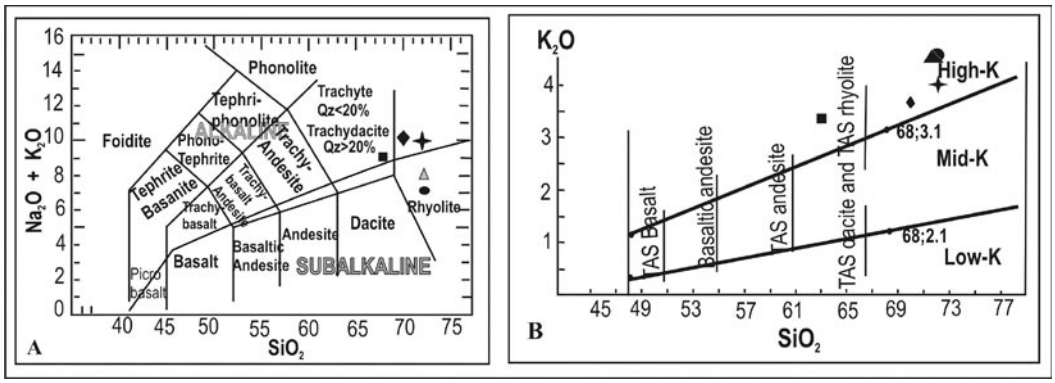

Figure 7. A. TAS chemical composition of Paipa volcano rocks. B. Peccerillo and Taylor chemical classification of Paipa volcano rocks. Selected samples are alkaline trachytes and rhyolites, and high-K calcalkaline rhyolites.

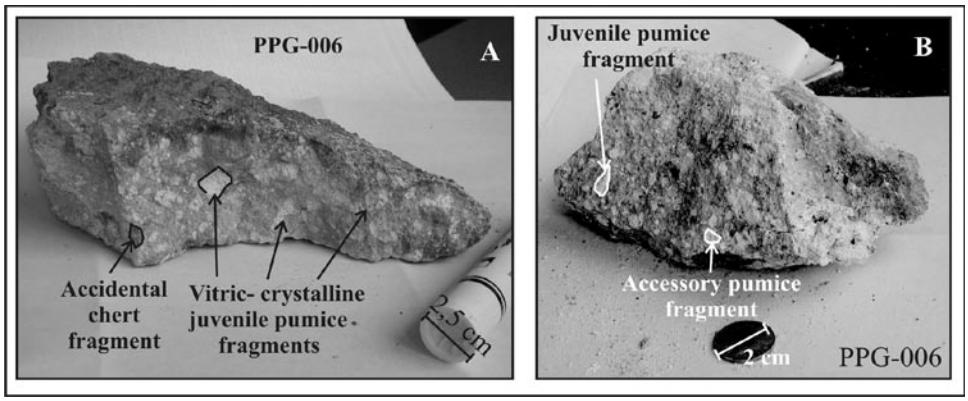

Figure 8. Hand samples from proximal outcrops of unit I.2, which is an ignimbrite. Pyroclastic rocks present flow textures with poorly sorted juvenile, accidental and accessory fragments in a vitroclastic brown to yellow matrix.

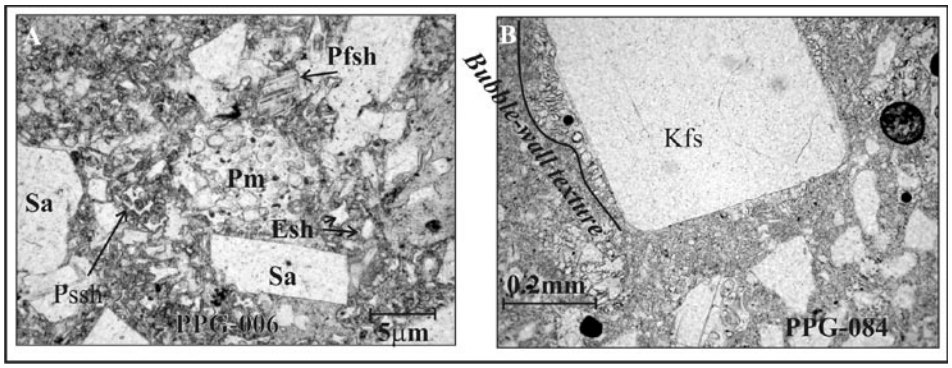

Figure 9. Unit I.2 pyroclastic flow tuffs. A. Juvenile rounded pumice fragments with spherical vesicles and angular sanidine crys□
shards are found. B. Vesicles are normal to crystal walls giving bubble-wall textures. Sa = sanidine; Kfs = juvenile anorthoclase crystal; Pm = juvenile pumice fragment; Pssh = Pumice shard with spherical vesicles; Pfsh = pumice shard with flatted vesicles; Esh = equant shards.

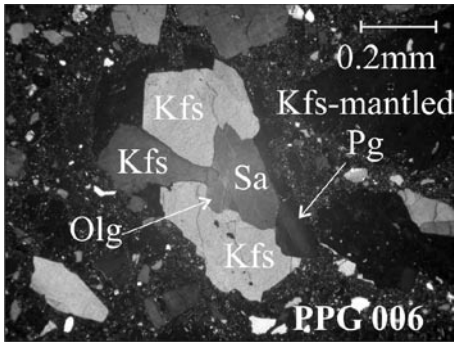

Figure 10. K-feldespar glomerocrysts.

Unit I.3 samples: the pumice and ash flow tuff cooling unit was sampled in PPG-005 GPS station, in El Guarrúz *puzzolana* mine (Figure 2). Hand samples are poorly sorted white pyroclastic flow tuffs, with abundant juvenile pumice fragments of different crystal content, up to 25-20% of armored lapilli (Figure 11) and up to 30 % of accidental metamorphic lithics in an ash and pumice matrix. In thin sections (Figure 12) these rocks were classified as vitric-lithic, with a combination of bubble-wall and pumice magmatic shards together with blocky and platy phreatomagmatic shards (Cepeda & Pardo-

Villaveces, 2004). Pumice vesicles are ellipsoidal and fibrous (Figure 12 B). Accidental lithics are dominant in field scale, as angular blocks and lapilli phylites, schists, red-yellow and green claystones, chert and quartzites; occasionally they are found in microscopic scale (ash sizes) and are mainly sub-rounded phylites and quartzites. Accessory lithics are crystalline vitric and vitric-crystal ash flow pyroclastic rocks, possibly detached from unit I.1 rocks. Modal composition is trachytic (Table 1) while chemical composition of sample PPG-005 suggests high-K cal-alkaline rhyolites (Figure 7).

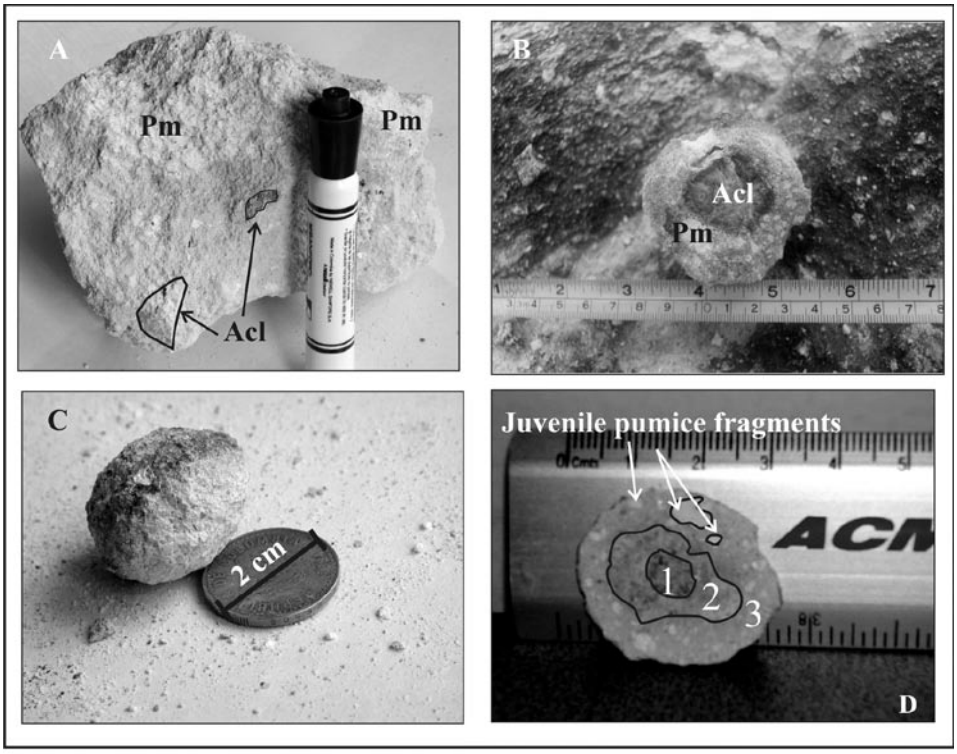

Figure 11. A. Hand sample of unit I.3 ignimbrites, composed of juvenile, accessory and accidental poorly sorted fragments in a vitroclastic matrix. B. Armored lapilli transversal section shows a metamorphic phylite as nucleus with a reaction border and a pyroclastic ash and pumice rim. C-D: armored lapilli can have more than two(2) layers; in this case 1 = accessory pumice as nucleus; 2 = intermediate layer of green ashes, Kfs crystals and pumice fragments. It has a corroded border. 3 = pumice and ash external regular sorted rim. Acc = Accidental lithic fragments; Pm = pumice fragment; Ml = accidental metamorphic lithic.

Unit I.4 samples: it is a pumice flow unit that was sampled in PPG-112 and PPG 113 GPS stations, in Los Morros *puzzolana* mine (Figure 2). Hand samples are white pyroclastic flow tuffs, with abundant highly vesiculated pumice fragments and accidental phylites and quartzites in a glassy matrix (Figure 13). In thin section (Figure 14) they are classified as vitric and vitric-crystalline flow tuffs (Figure 5) with occasional plagioclase, anorthoclase and sanidine free phenocrysts in a vitroclastic matrix. Bubbles present different morphologies from spherical to strongly elongated; some fragments are fibrous with tube-like bubbles, shards are mainly bubble-wall type and vesicles tend to surround crystals normal to crystal faces, giving a bubble-wall texture (Figure 14). Modal classification (Table 1) indicates K-feldspar trachytes.

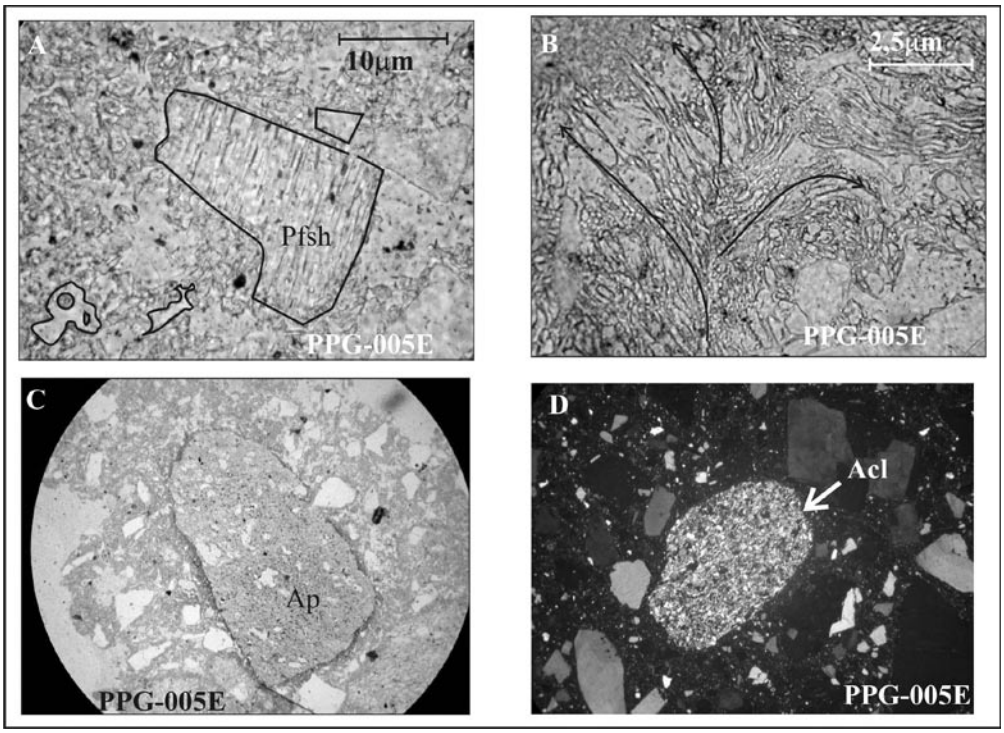

Figure 12. A. Pyroclastic textures of Unit I.3 ignimbrites, with abundant equant fragments with flattened vesicles, without vesicles and pumice bubble-wall shards. B. Vesicles range in morphology from complete spherical to fibrous and show directional flow. Deformation causes pull-apart textures. C. Accessory lithics are sub-rounded altered pumice fragments while D accidental lithics are mainly metamorphic. Pfsh = pumice shard with flattened vesicles; Ap = accessory pumice fragment; Acl = accidental lithic (here: phylite).

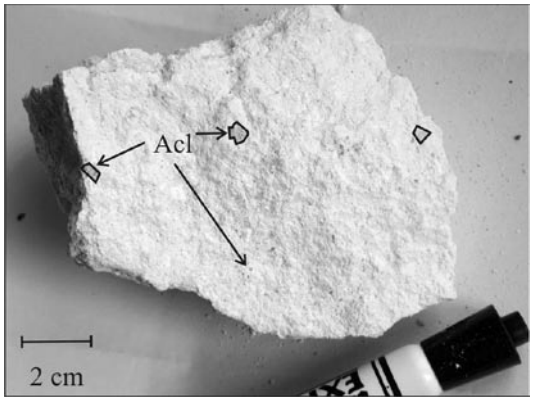

Figure 13. Pyroclastic flow tuffs of unit I.4 are mainly vitric with occasional accidental quartzites, green and yellow phyllites. Acl = accidental lithics.

Unit II.1 samples: lava-dome rocks, sampled in PPG-069, PPG-070, PPG-104 and PPG-119 GPS stations, are hypocrystaline gray rocks, with anorthoclase phenocrysts up to 1,5 cm (Figure 15). In thin section (Figure 16) some of these phenocrysts are pokilocrysts with an oligoclase nucleus (Figure 16 B). Feldspar free crystals and glomerocrysts are surrounded by red-microfolded biotite crystals which give a flow texture to the rocks (Figure 16 B and D). In the glassy matrix there were identified finer crystals of anorthoclase, hastingsite, oxihornblende and sphene. The finer anorthoclase microcrystals show penetration cracks and hollow nucleus with occasional glass inclusions (Figure 16 I). Modal (Table 1) and chemical classification (Figure 7) indicate alkaline affinity trachytes with less than 20% normative quartz. Sample M-119i, taken at Honda Grande Creek dome, is alkaline rhyolitic in composition (Figure 7); augite-aegirinae was identified as an accessory mineral (Figure 16 J-K), and β-quartz as a trace mineral.

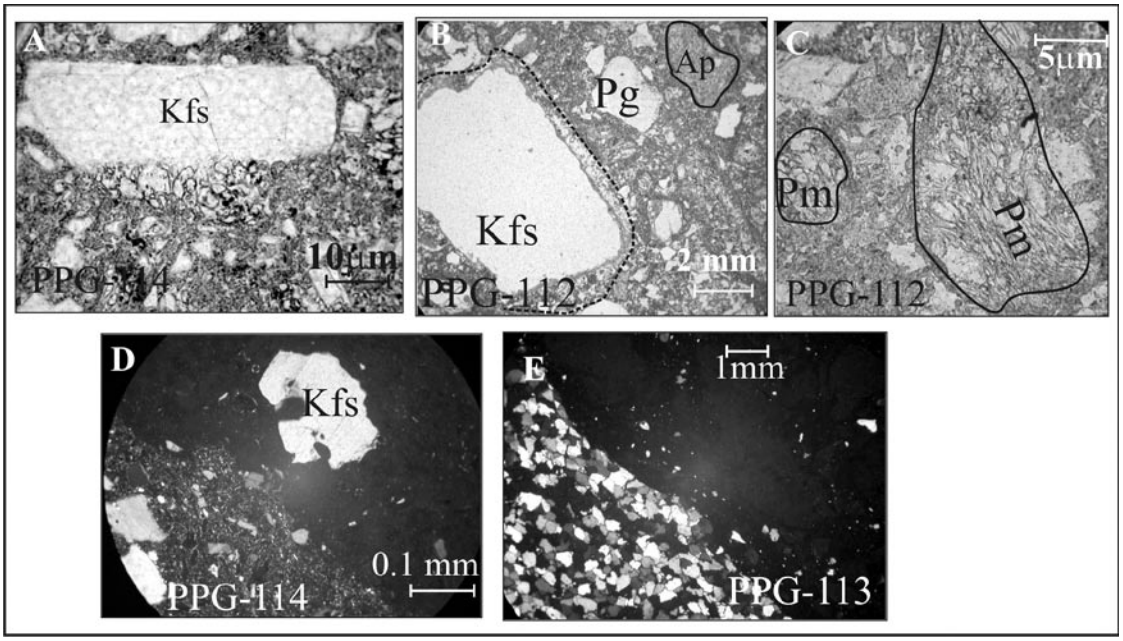

Figure 14. Pyroclastic textures of unit I.4 flow tuffs. Bubble-wall textures are common (A and B) around anorthoclase phenocrystals. The main constituents of the rock are juvenile pumice fragments without crystals in the (C). Rocks are mainly vitric tuffs with occasional feldespars showing dissolution embayments (D). Accidental lithic fragments are angular phyllites and quartzites (E). Kfs = Anorthoclase. Pg = plagioclase. Pm = juvenile pumice. Ap = accessory pumice fragment.

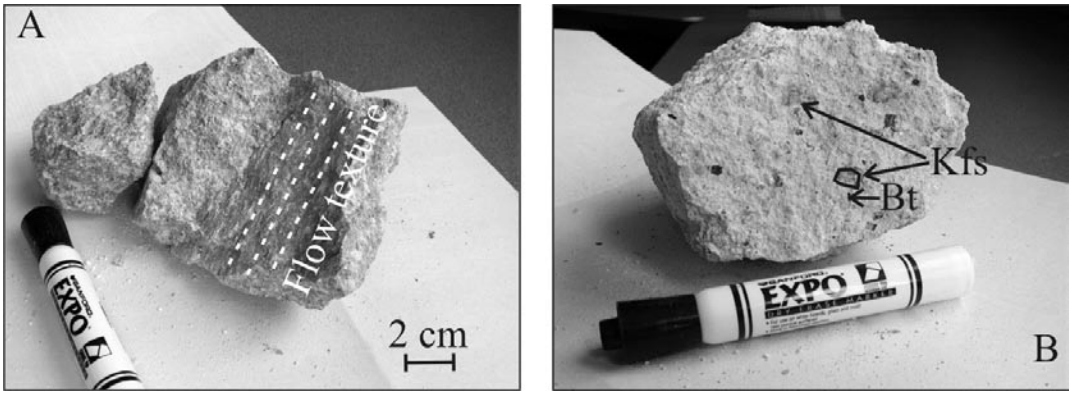

Figure 15. A. Rock fragment of Olitas lava-domes. Anorthoclase, oligoclase, albite and red biotite are aligned and oriented suggesting a flow direction. B. Rock fragment of Honda Grande Creek dome. Mafics are hastingsites, augite-aegirine and red biotite. Fe-oxides tend to alter crystals.

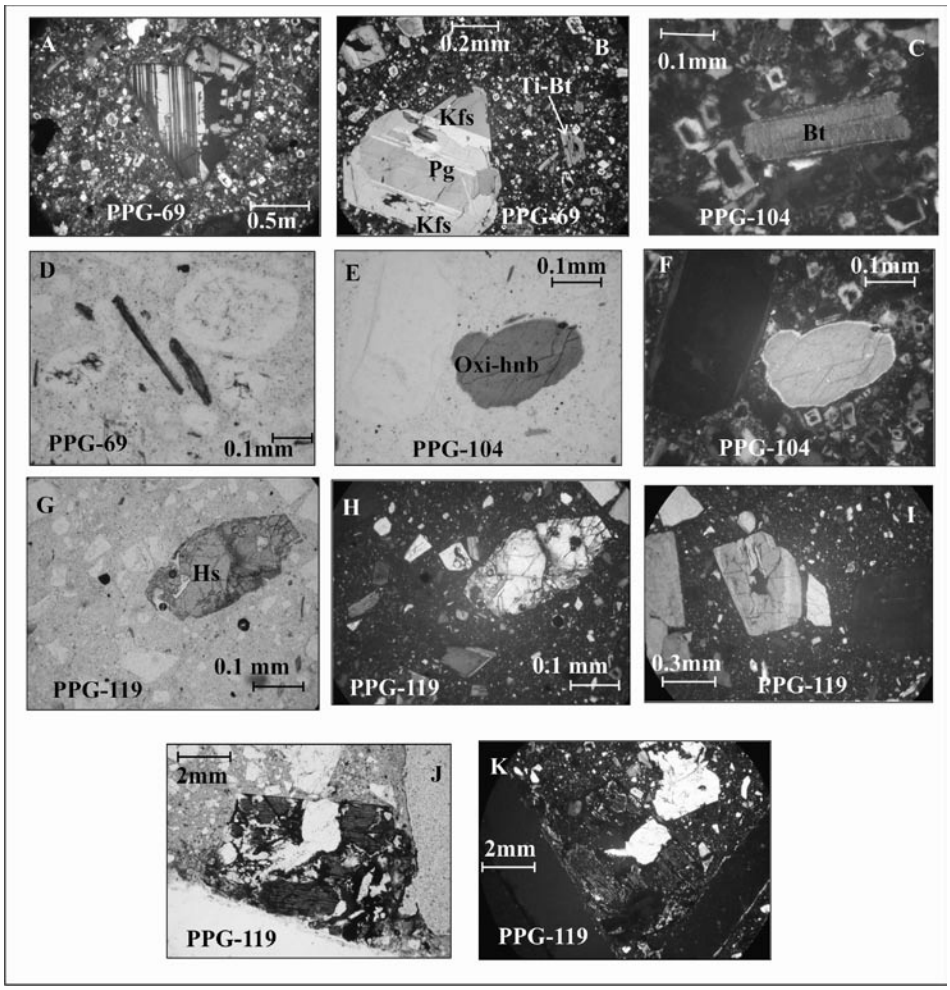

Figure 16. A. Plagioclase is albite and oligoclase in composition, it is commonly twinned and zoned. B. Some plagioclase crystals are mantled by potassic feldespar (anorthoclase) and form glomerocrystals. C. The main mafic mineral is red biotite. In this thin section Kfs microcrystals are visible, all of them wit a hollow nucleus. D. Commonly, red biotites are folded. E-F. high b
have the hollow nucleus and penetration cracks. J-K. Green augite-aegirine occurs as mafic accessory mineral.

In summary, figure 7, tables 2 and 3 show chemical data of the five selected samples, which are mainly alkaline trachytes and rhyolites. The oldest rocks are the most silicic rocks (72%) and less aluminous (16%) while the younger are less silicic (68%) and more aluminous (18%). In general, all samples have high contents of alkalis (7-10%), in which Na content is greater than K content, which is consistent with anorthoclase, Na-amphibole and Na-Pyroxene crystallization. On the other hand, TiO_2 content (< 0,33%) was enough for red-biotite crystallization as an accessory mineral, and sphene as trace mineral. Composition is confirmed by other 10 rocks sampled during INGEOMINAS Colombia Geochemical map project (in Cepeda & Pardo-Villaveces 2004). Chemical data were processed to calculate CIPW norm and to estimate the physical conditions of magma reported in table 4.

TABLE 2. RECALCULATED WHOLE ROCK MAJOR ELEMENTS CHEMICAL DATA.

SAMPLE	SiO_2	Al_2O_3	Na_2O	K_2O	CaO	Fe_2O_3	FeO	MgO	TiO_2	P_2O_5
119i	70,5	16,44	6,7	3,65	0,41	1,26	0,85	0,05	0,15	0,00
069i	68,2	18,05	5,91	3,43	0,83	2,03	0,67	0,50	0,24	0,10
084i	72,2	17,26	2,69	4,64	0,30	1,68	0,77	0,14	0,33	0,00
005E	72,0	16,77	3,85	4,59	0,24	1,43	0,66	0,11	0,26	0,11
102i	71,6	16,2	6,67	3,71	0,17	0,77	0,71	0,02	0,13	0,00

TABLE 3. ÁLCALIS % VS. SILICA %: CHEMICAL CLASSIFICATION (FOR TAS DIAGRAM IN FIGURE 7).

SAMPLE	Na_2O+K_2O	SiO_2	
119i	10	70,5	♦
069i	9	68,2	
084i	7	72,2	o
005E	8	72,0	Δ
102i	10	71,6	★

In order to confirm the obtained composition we compare our five sample analysis with ten other major oxides chemical data (Table 5) determined by INGEOMINAS "Colombia geochemical map" project to support our observations (Cepeda & Pardo-Villaveces, 2004; Güiza & Muñóz, 2005). Rhyolitic and trachytic composition for Paipa volcano products are confirmed and shown in Figure 17.

DISCUSSION

Rocks textures suggest an intratelluric environment in which crystals grew rapidly under various nucleation rates, promoting twinned forms, (Pg in Figure 3A, Hs in Figure 3C, Pg in Figure 16 A, Pg and Kfs in Figure 16 B) and a former viscous melt in which cation diffusion was difficult. While differentiation took place, there was no chemical and no physical equilibrium between plagioclase and hastingsite crystals and the melt, as suggested by dissolution texture, reabsortion and reaction borders (Figures 6A, 6B, 6E, 14D). Plagioclase and oxi-hornblende rounding (Figures 3B, 16E and 16F) could be the result of the convective currents that transport crystals in a possibly thermally stratified magmatic chamber; otherwise it could be the result of system reheating due to hotter magma injection at the base of the chamber (Pardo-Villaveces, 2004).

High growing rates together with low nucleation and low diffusion rates favored feldspar movement along compositional boundaries without reaching the equilibrium, producing compositional and textural zonation: anorthite to albite transformation was faster than growing and crystallization, originating normal-zoned crystals. Some crystals show fibrous rings alternated with euhedral rims, which represent adjustment periods to new thermodynamic and compositional conditions (Figure 6 C and 6D).

On the other hand, anorthoclase poikilocrysts with plagioclase nucleus (Figures 3A and 6F) suggest the following hypothesis (Pardo-Villaveces, 2004): (1) following Carmichael et al. (1974), anorthite-poor melts in the water-saturated $NaAlSi_3O_8$- $KAlSi_3O_8$ -SiO_2 subsystem, can crystallize progressively more sodic feldspars that, later, become more potassic. This fact results in progressively more sodic sanidines and anorthoclase overgrowing around corroded plagioclase. (2) Fast nucleation plagioclase could get trapped into the slower coeval anorthoclase growth. (3) Mixing of trachytic and rhyolitic magmas and/or mixing of magmas of different alkalinity.

Water introduction could depolimeryzed magma, increasing diffusion and nucleation rates with heat loss and volatile release, allowing the generation of a second generation of alkaline feldspars (Figures 3 C, 6B, 16 A and 16 C).

TABLE 4. CIPW NORM. RESULTS GIVEN BY NORMA.XSL. DIFFERENTIATION INDEX, ESTIMATED MELT TEMPERATURES AND VISCOSITY (LOGη) WERE CALCULATED BY THE SOFTWARE.

Sample	Normative mineral	weight %	vol %	QAP vol%	Fe3+/total Fe	Mg/ (Mg+ total Fe)	Mg/(Mg+Fe2+) in the rock	Mg/(Mg+Fe2+) in silicates	Ca/(Ca+Na)	Ca/(Ca+Na) in plagioclase	Differentation index	Calculated density, g/cc	Calculated melt density	Calculated viscosity (Dry)	Calculated viscosity (wet)	Estimated melt T°	Estimated water content
005E	**Quartz**	31.66	32.2	**34**	**66.1**	**9.2**	**22.9**	**100**	**3.3**	**1.3**	**91.8**	**2.7**	**2.38**	**9.7**	**7.3**	**811**	**3.7**
	Orthoclase	27.13	28.56	**30**													
	Plagioclase	33.05	33.97	**36**													
	Hyperstene	0.27	0.23														
	Magnetite	1.37	0.71														
	Ilmenite	0.49	0.28														
	Hematite	0.48	0.25														
	Corindon	5.29	3.59														
	Apatite	0.25	0.21														
069i	**Quartz**	18.48	18.8	**20**	**73.2**	**26.3**	**57.1**	**100**	**7.2**	**6.1**	**92.2**	**2.69**	**2.4**	**7.8**	**6.2**	**879**	**2.95**
	Orthoclase	20.27	21.34	**22**													
	Plagioclase	53.47	54.82	**58**													
	Hyperstene	1.25	1.05														
	Magnetite	1.46	0.46														
	Ilmenite	0.46	0.26														
	Hematite	1.02	0.52														
	Corindon	3.36	2.27														
	Apatite	0.23	0.2														
084i	**Quartz**	37.93	38.97	**42**	**66.3**	**9.9**	**24.5**	**100**	**5.8**	**5.8**	**89.6**	**2.72**	**2.39**	**10.1**	**7.6**	**807**	**3.74**
	Orthoclase	27.42	29.16	**31**													
	Plagioclase	24.25	25.12	**27**													
	Hyperstene	0.35	0.3														
	Magnetite	1.53	0.8														
	Ilmenite	0.63	0.36														
	Hematite	0.63	0.33														
	Corindon	7.27	4.97														
102i	**Quartz**	18.01	17.97	**19**	**49.4**	**2.5**	**4.8**	**12.6**	**1.4**	**1.4**	**97.2**	**2.64**	**2.37**	**8.9**	**6.7**	**817**	**3.63**
	Orthoclase	21.92	22.64	**23**													
	Plagioclase	57.28	57.75	**59**													
	Hyperstene	0.5	0.34														
	Magnetite	1.12	0.57														
	Ilmenite	0.25	0.14														
	Corindon	0.9	0.6														
119i	**Quartz**	16.47	16.48	**17**	**57.2**	**4.3**	**9.5**	**37.5**	**3.3**	**3.3**	**96.8**	**2.65**	**2.38**	**8.4**	**6.5**	**838**	**3.4**
	Orthoclase	21.57	22.34	**22**													
	Plagioclase	58.73	59.32	**61**													
	Hyperstene	0.4	0.29														
	Magnetite	1.83	0.93														
	Ilmenite	0.28	0.16														
	Corindon	0.72	0.48														

The results given by norma.xsl software suggest highly differentiated rocks (DI varies between 89 and 97%), low melt density (between 2, 37 a 2, 4 g/c^3), high viscosity (given as log η = 8, 9 a 10, 1 for FEE rocks and 7, 8 to 8, 4 for the SEE domes) and melt temperatures between 807 and 879ºC.

TABLE 5. GEOCHEMICAL DATA OBTAINED BY INGEOMINAS "COLOMBIA GEOCHEMICAL MAP" PROJECT. BY GÜIZA & MUÑÓZ, 2005.

Sample*	SiO_2	Al_2O_3	Fe_2O_3	CaO	MgO	Na_2O	K_2O	TiO_2
	%	%	%	%	%	%	%	%
11	72.1230979	16.9501905	1.40469212	0.32892669	0.1593778	3.8287366	4.84989806	0.35508034
12	71.881809	16.76715	1.72385273	0.39979945	0.19292122	3.877437	4.81598419	0.34104632
13	71.8887409	17.1697144	1.29146806	0.33121514	0.14265479	3.6669538	5.12976548	0.37948745
18	69.1726451	18.0063316	1.55751126	0.15344514	0.12722136	2.42267076	1.74277728	0.44633945
19	72.2317757	16.7512619	1.54303488	0.22806073	0.08441302	6.17504981	4.4887606	0.28722781
22	71.5781045	16.034841	3.88164253	0.38545421	0.14609375	3.96315871	4.64318143	0.33603944
24	68.2734892	18.6174059	2.71293447	0.25446071	0.13185836	3.70521606	2.2989253	0.46571028
26	68.4212936	18.109168	1.66899817	0.53131542	0.17480699	4.73142071	3.93664664	0.29993027
29	69.1846068	18.0984763	1.74764919	0.59975306	0.15983205	6.76990757	3.61231267	0.29830139
30	68.2665033	18.0854095	2.13505852	0.17759233	0.09561156	3.8390687	2.16706	0.39659694

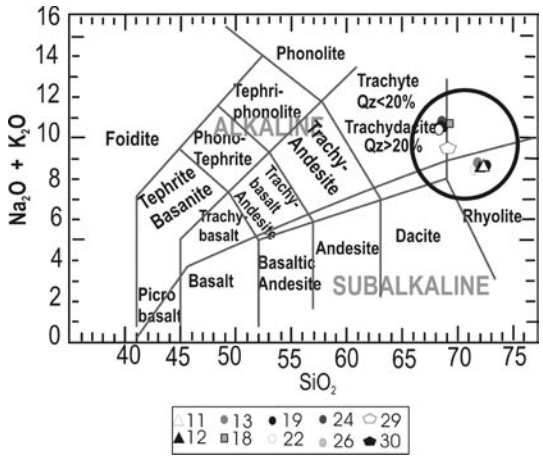

Figure 17. TAS diagram showing classification of ten samples based on geochemical data obtained by INGEOMINAS "Colombia geochemical map" project (Cepeda & Pardo-Villaveces, 2004; Güiza & Muñóz, 2005).

Once magma encountered one or several conduits, its interaction with external water, as suggested by phreatomagmatic shards, surface pitting and abundance in lithics, reported in Cepeda & Pardo-Villaveces (2004) caused explosive fragmentation and the first eruption known for Paipa volcano (Pardo-Villaveces & Alfaro, 2005). Eruption columns did not reach enough height and pyroclastic flows were originated by their continuous collapse (Pardo-Villaveces et al., 2005). A former pyroclastic edifice was formed this way, whose eroded walls still evident in the field (Figure 18). In this way, the last solidifying phase was the glass and its composition represents the composition of the viscous residual silicic melt, where quartz could not crystallize because of the difficult ion diffusion or because during magma differentiation and feldspar crystallization, eutectic conditions were not reached.

After an erosion or no-depositional period inferred by the stratigraphy reported in Pardo-Villaveces et al. (2005), magma could rise again along the conduit (s) and suffered volatile saturation and exolusion by the lower pressure; system disruption, due to magma injection, volatile introduction or sudden decompression, enhanced the transformation of a melt of liquid, solid crystals and dissolved gasses into a mixture of gasses with liquid drops and solid fragments; melt density reduction (expansion) resulted in a rapid acceleration through and out of the vent, detonating further eruptions (Unit I.2). Magmatic fragmentation processes allowed vesicle formation and coalescence, particularly around and perpendicular to crystal borders (Figure 9 B). Bubble inner pressure excess generated bubble wall thinning until the complete rupture, forming glass shards and larger vesicles (Figure 9 A).

A third eruptive unit was deposited after an explosive interaction between magma and meteoric water (phreatomagmatic eruption. Pardo-Villaveces et al., 2005); pumice fragments were randomly distributed in a vitroclastic matrix with abundant blocky shards, vesiculated and not vesiculated shards (Figure 12 A). Rounded and ellipsoidal vesicles grew spherically and then were plastically deformed in the viscous flow along the conduit (Figure 12 B). The high input of dense lithic fragments enhanced column collapse and wet conditions allowed the formation of armored lapilli rich pyroclastic flows. Cepeda & Pardo-Villaveces (2004) proposed a combination of

magmatic and phreatomagmatic mechanisms. After a quiescence period, bubble nucleation around crystalline faces developed *pull-apart* textures (Figure 12 B) due to the greater effort under rapid exolusion and expansion. Foam was formed in the magma until it boiled over the vent, generating a small lobe of vitric flow tuffs over the northeastern edifice flank (Pardo-Villaveces, 2004. Pardo-Villaveces et al., 2005).
Based on Pardo-Villaveces (2004), Cepeda & Pardo-Villaveces (2004) and Pardo-Villaveces et al. (2005) we know that a caldera resurgence that began during the SEE with conduit opening and alkaline trachytic to rhyolitic magma emission near the caldera margins; initial volcanism was not explosive in nature: magma could reach the surface after complete volatile release through conduit permeable walls, promoting anorthoclase and sanidine nucleation rate increment and amphibole and mica stability reduction, which generated corrosion and opatization borders in mafics. Thermodynamic and compositional disequilibrium was permanent leading to the formation of dissolution embayments, reabsortion borders, normal, inverse and oscillatory plagioclase zonation (Figure 16) (Pardo-Villaveces, 2004).

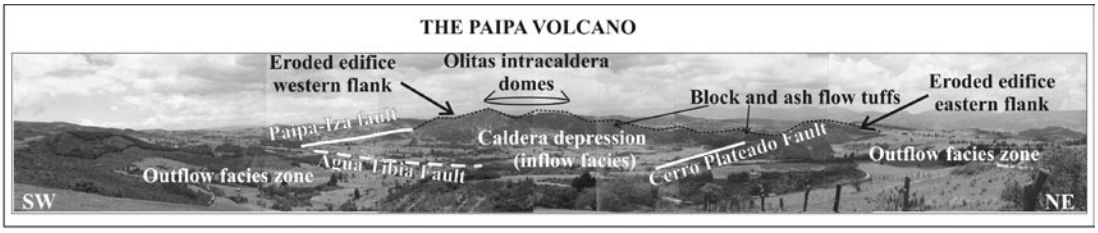

Figure 18. The Paipa Volcano has a 3 Km-diameter caldera with several vents inside it, most of them located at Olitas headstream. Outflow facies are mainly ignimbrites while inflow facies are block and ash flows, ignimbrites, surges, domes, sedimentary high energy and low energy deposits (Pardo-Villaveces et al., 2005).

SUMMARY AND CONCLUSIVE REMARKS

The Paipa volcano produced alkaline rhyolitic and trachytic to high-K calcalkaline rhyolitic magmas eruptions during the Pliocene. Calculated differentiation index (DI) varies between 89 and 97%, while calculated melt density oscillates between 2, 37 a 2, 4 g/c^3 (low). Viscosity is relatively high (log η = 8, 9 a 10, 1 for FEE rocks and 7, 8 to 8, 4 for the SEE domes) and temperatures were estimated between 807 and 879ºC. Under different nucleation, diffusion and growing rates, augite-aegirine, sphene, zircon, oligoclase, anorthoclase and sanidine could crystallize in the intratelluric environment. Water content allowed hydrous-phases crystallization, such as hastingsite and biotite, and it was a dominant factor in magma explosivity and in eruptive mechanisms. Most of the feldspars and amphiboles show evidences of thermodynamic and compositional disequilibrium with the melt, as indicated by dissolution embayments, different kinds of zonation, reabsortion and corrosion borders.

Together with the published data of Iza volcanic rocks (Boyaca) the alkaline and silica-rich magmas that were erupted in the eastern Cordillera during the Pliocene are strongly distinct from the calcalkaline magmas of the Central Cordillera, which suggest different geotectonic conditions. While the active arc is clearly related to the subduction of Nazca Plate under South America, we still don't know the origin of the Eastern Cordillera magmas and their volcano-tectonic framework.

RECOMMENDATIONS

Since the geotectonic environment and the relation between volcanism and the Eastern Cordillera regional compressive regime are not well understood, exhaustive geochemical and petrologic studies, together with structural, geophysical, seismic, tectonic and detailed geochronology research still have to be done. It would help to clarify petrogenesis and magma evolution through the continental crust.

REFERENCES

- Carmichael I., Turner F., Verhoogen J. Crystallization paths of igneous minerals at low pressures. 1974. Igneous Petrology. Chapter 5. Mc Graw Hill. International series of Earth Sciences. 739 p
- Cepeda H. & Pardo-Villaveces N., 2004. Vulcanismo de Paipa. Informe técnico del INGEOMINAS. INGEOMINAS-Bogotá. Colombia. 140 p.
- Cepeda H., Pardo-Villaveces N., Jaramillo J. 2004. The Paipa Volcano, Colombia, South America. Abstract in IAVCEI meeting. November 14-19, Pucón, Chile.
- Güiza S., Muñoz R. 2005. Blancos de mineralización teletermal asociados a vulcanismo en la región de Paipa . Boyacá. Memorias X Congreso Colombiano de Geología.
- Wohletz K., & Heiken G. 1992, Volcanology and Geothermal Energy. University of California Press, Berkeley, CA, 432 pp.
- Le Maitre, R. W. (1989). A Classification of Igneous Rocks and Glossary of Terms: Recommendations of the International Union of Geological Sciences, Subcommission on the Systematics of Igneous Rocks. Oxford: Blackwell, 193 pp
- Martínez A., 1989. Geologie de la Region D'Iza, Boyacá. Cordillere Orientale de Colombie. Diplome de mineralogie et geologie. Instituts de Mineralogie et Geologie, Universite de Lusanne, Nov. 200 p.
- Pardo-Villaveces N., 2004. Estratigrafia de las vulcanitas asociadas al volcán de Paipa, municipios de Paipa y Tuta, Departamento de Boyacá. Colombia. Tesis de grado Universidad Nacional de Colombia-Bogotá. 190 p.
- Pardo-Villaveces N., Alfaro, C. 2005. Caracterización de cenizas volcánicas por microscopio electrónico para determinación de mecanismos eruptivos. Caso Volcán de Paipa, Boyacá. Memorias X Congreso Colombiano de Geología, Bogotá.
- Pardo-Villaveces N., Cepeda H., Jaramillo J.M. 2005. The Paipa Volcano, Eastern Cordillera of Colombia (Part I) : Volcanic stratigraphy. *Submitted to the Earth Sciences Research Journal for evaluation*.
- Peccerillo A. & Taylor T.S. 1976. Geochemistry of Eocene calc-alkaline volcanic rocks from Kastamonu area,

Northern Turkey. Contrib. Mineral. Petrol., 58, 63-81.

- Streckeisen, A. (1978). Classification and nomenclature of volcanic rocks, lamprophyres, carbonatites and melilitic rocks: recommendations and suggestions, IUGS Subcommission on the Systematics of Igneous Rocks. *Neues Jahrbuch für Mineralogie, Abhandlungen* 134, 1–14.